The Company of Biologists

STEM CELLS AND REGENERATION

RESEARCH ARTICLE

Re-epithelialization of cutaneous wounds in adult zebrafish combines mechanisms of wound closure in embryonic and adult mammals

Rebecca Richardson[1,*,¶,**], Manuel Metzger[1,¶], Philipp Knyphausen[1,2], Thomas Ramezani[1,‡], Krasimir Slanchev[3,§], Christopher Kraus[1], Elmon Schmelzer[4] and Matthias Hammerschmidt[1,5,6,**]

ABSTRACT

Re-epithelialization of cutaneous wounds in adult mammals takes days to complete and relies on numerous signalling cues and multiple overlapping cellular processes that take place both within the epidermis and in other participating tissues. Re-epithelialization of partial- or full-thickness skin wounds of adult zebrafish, however, is extremely rapid and largely independent of the other processes of wound healing. Live imaging after treatment with transgene-encoded or chemical inhibitors reveals that re-epithelializing keratinocytes repopulate wounds by TGF-β- and integrin-dependent lamellipodial crawling at the leading edges of the epidermal tongue. In addition, re-epithelialization requires long-range epithelial rearrangements, involving radial intercalations, flattening and directed elongation of cells – processes that are dependent on Rho kinase, JNK and, to some extent, planar cell polarity within the epidermis. These rearrangements lead to a massive recruitment of keratinocytes from the adjacent epidermis and make re-epithelialization independent of keratinocyte proliferation and the mitogenic effect of FGF signalling, which are only required after wound closure, allowing the epidermis outside the wound to re-establish its normal thickness. Together, these results demonstrate that the adult zebrafish is a valuable *in vivo* model for studying and visualizing the processes involved in cutaneous wound closure, facilitating the dissection of direct from indirect and motogenic from mitogenic effects of genes and molecules affecting wound re-epithelialization.

KEY WORDS: FGF, Re-epithelialization, Skin, TGF-β, Wound healing, Cell proliferation

INTRODUCTION

The epidermis, which is composed of specialized epithelial cells called keratinocytes, protects the body from injury and invading pathogens (Presland and Jurevic, 2002). Therefore, damage to the epidermis must be promptly repaired to restore this essential barrier. Vertebrate organisms have developed varying mechanisms for wound closure and re-epithelialization by keratinocytes. Studies in embryonic mouse models have revealed an ability to rapidly re-epithelialize small skin wounds in the absence of strong inflammatory responses, involving the planar cell polarity (PCP) system regulating actin polymerization and keratinocyte polarity, as well as contractions of an actomyosin cable in the leading edge (LE) keratinocytes (Bement et al., 1993; Brock et al., 1996; Caddy et al., 2011; Cowin et al., 1998; Hopkinson-Woolley et al., 1994; Longaker et al., 1990; Martin and Lewis, 1992). By contrast, wound healing in adult mammals is a complex, multi-step process involving blood clot formation, inflammation, re-epithelialization by keratinocyte crawling and proliferation, granulation tissue formation, neovascularization and tissue contraction, which largely overlap in time (Barrientos et al., 2008; Martin, 1997; Shaw and Martin, 2009; Singer and Clark, 1999; Werner and Grose, 2003).

Studies in mammalian systems have further demonstrated that re-epithelializing keratinocytes are regulated by various cytokines and growth factors secreted by the damaged tissue or other participating cell types (Barrientos et al., 2008; Santoro and Gaudino, 2005; Sivamani et al., 2007; Werner and Grose, 2003). However, as a result of the temporal overlap of the various processes, it can be difficult to dissect direct effects on keratinocytes from indirect effects via other involved cell types, as well as the impact on keratinocyte migration versus proliferation.

In mice, fibroblast growth factors (FGFs) with direct effects on keratinocytes are FGF7 (also known as keratinocyte growth factor, KGF) and its close relative FGF10, which act through high-affinity binding to the receptor splicing variant FGFR2IIIb that is found only in keratinocytes (Barrientos et al., 2008). Accordingly, transgenic mice expressing a dominant negative, truncated version of FGFR2IIIb in keratinocytes display a severe delay in wound re-epithelialization, coincident with strongly reduced keratinocyte proliferation at the edges of the wounds (Werner et al., 1994), pointing to an essential mitogenic effect of FGF7/10 signalling. However, concomitant motogenic effects of FGF signalling on keratinocyte migration, as for instance revealed in cell culture systems, cannot be ruled out (Barrientos et al., 2008; Meyer et al., 2012).

Data on the role of transforming growth factor beta (TGF-β) signalling during wound closure are conflicting. In cell culture systems, TGF-β1 stimulates keratinocyte migration, possibly by inducing (partial) epithelial-mesenchymal transitioning (EMT), by promoting protrusive activity (Lamouille et al., 2014; Räsänen and Vaheri, 2010; Weber et al., 2012) and/or by shifting integrin populations in LE keratinocytes towards a more migratory

[1]Institute of Developmental Biology, University of Cologne, Cologne D-50674, Germany. [2]Graduate School for Biological Sciences, University of Cologne, Cologne D-50674, Germany. [3]Georges-Koehler Laboratory, Max-Planck Institute of Immunobiology and Epigenetics, Freiburg D-79108, Germany. [4]Cell Biology, Max-Planck Institute for Plant Breeding Research, Cologne D-50829, Germany. [5]Center for Molecular Medicine Cologne, University of Cologne, Cologne D-50931, Germany. [6]Cologne Excellence Cluster on Cellular Stress Responses in Aging-Associated Diseases, University of Cologne, Cologne D-50931, Germany. *Present address: Department of Physiology and Pharmacology, School of Medical Sciences, University of Bristol, Bristol BS8 1TD , UK. ‡Present address: MRC Centre for Inflammation Research, The Queen's Medical Research Institute, Edinburgh EH16 4TJ, UK. §Present address: Max-Planck Institute of Neurobiology, Martinsried D-82152, Germany.
¶These authors contributed equally to this work

**Authors for correspondence (rebecca.richardson@bristol.ac.uk; mhammers@uni-koeln.de)

M.H., 0000-0002-3709-8166

DEVELOPMENT

phenotype (Gailit et al., 1994; Li et al., 2006; Margadant and Sonnenberg, 2010; Zambruno et al., 1995). However, *in vivo* data do not fully support such a stimulatory role of TGF-β signalling. Thus, mouse null mutants for *Tgfb1* or the TGF-β-regulated transcription factor *Smad3* show accelerated, rather than impaired wound closure (Ashcroft et al., 1999; Koch et al., 2000). This paradoxical result has been proposed to be due to concomitant and predominant effects of TGF-β signalling to suppress keratinocyte proliferation, which might counteract a direct stimulatory effect on epidermal migration (Ashcroft et al., 1999; Barrientos et al., 2008; Sivamani et al., 2007).

Here, we examine *in vivo* wound closure in adult zebrafish, analysing and dissecting the cellular mechanisms underlying the re-epithelialization of full-thickness (Richardson et al., 2013) and partial-thickness wounds. Using chemical treatments combined with *in vivo* imaging, we show that re-epithelialization utilizes TGF-β/integrin-dependent active keratinocyte crawling at the LE of the recovering epidermis, as well as epidermal re-arrangements, including cellular intercalations that progressively spread into more distant regions and lead to a reduction of epidermal cell layers, thereby providing the keratinocytes to populate the wound. However, re-epithelialization of adult zebrafish wounds is independent of FGF signalling and cell proliferation, which are only required for later remodelling and re-establishment of the epidermis outside the wound, exemplifying how the zebrafish system can be used to dissect mitogenic versus motogenic effects of growth factors on re-epithelializing keratinocytes *in vivo*.

RESULTS
Re-epithelialization of cutaneous wounds is extremely rapid

We studied re-epithelialization of both full- and partial-thickness cutaneous wounds. Circular full-thickness wounds of ~1 mm or 2 mm in diameter were introduced onto the flank of adult zebrafish with a dermatology laser, ablating tissue to the level of the subcutaneous muscle layer (Richardson et al., 2013) (Fig. 1A,C). Partial-thickness wounds still containing the basal-most dermal layer were generated by manual removal of single scales (Fig. 1A,B). Time-lapse *in vivo* imaging of *Tg(krt4:GFP)* fish, where the superficial epidermal cells are labelled with GFP, revealed that partial-thickness wounds close very rapidly with a speed of ~500 µm/h (Fig. 1D), in line with previously reported rates for partial-thickness wounds in the cichlid fish *Hemichromis bimaculatus* (Quilhac and Sire, 1999). By contrast, full-thickness wounds closed more slowly (~250 µm/h; Fig. 1E); particularly in central wound regions where the wound bed is deeper and more uneven. Immunofluorescence analysis demonstrated that in contrast to unwounded epidermis, which is composed of three to four cell layers (Fig. 1F), and in contrast to the neo-epidermis at later stages, which is up to 10 cell layers thick (see below), the re-epithelializing epidermis was initially bi-layered, composed of GFP$^+$ superficial cells and p63$^+$ inner keratinocytes (Fig. 1G,H). Of note, full-thickness wounds were mainly re-epithelialized from the posterior side, although movement and elongation of keratinocytes was observed both on the anterior and posterior side (Movie 1; Fig. S1B,C). However, on the anterior side, keratinocytes
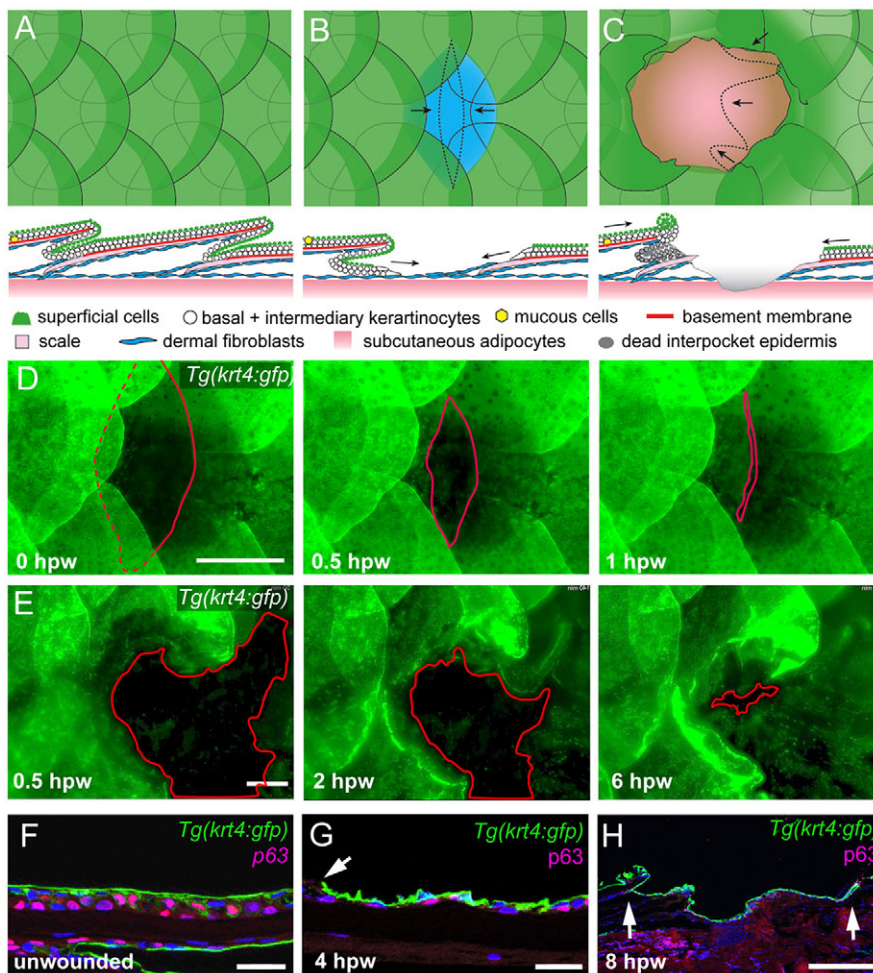

Fig. 1. Re-epithelialization of full- and partial-thickness wounds in adult zebrafish.
(A-C) Schematic representations of normal adult zebrafish skin architecture (A), or following partial-thickness (B) or full-thickness (C) wound introduction. Arrows in B and C indicate the typical directions of epidermal re-epithelialization. (D,E) Single images from time-lapse recordings of *Tg(krt4:GFP)* fish following partial-thickness (D) or full-thickness (E) wounding at indicated time points post-wounding; red line marks LE. (F-H) Unwounded epidermis is 3-4 cell layers thick (F), the re-epithelializing neo-epidermis is bilayered, consisting of superficial GFP$^+$ and inner p63$^+$ keratinocytes (G,H). Arrow in G indicates LE, arrows in H, the wound margins, revealing full re-epithelialization at 8 hpw. Scale bars: 500 µm in D,E,H; 20 µm in F,G.

Legend: ■ superficial cells | ○ basal + intermediary keratinocytes | ○ mucous cells | ▬ basement membrane | □ scale | — dermal fibroblasts | ■ subcutaneous adipocytes | ● dead interpocket epidermis

accumulated at the tips of the scale remnants (Fig. S1A), whereas on the scale-free head, wounds were re-epithelialized from both sides and in a more concentric fashion (Fig. S1D).

The leading edge: purse-string mechanisms and active keratinocyte migration

Cutaneous wounds of mammalian embryos close via purse-string mechanisms, involving coordinated actomyosin-dependent concentric constrictions of the epidermal sheet at the edge of the wound (Brock et al., 1996; Martin and Lewis, 1992), whereas closure of wounds in adult mammals involves active cell migration of keratinocytes. Zebrafish embryos also utilize purse-string mechanisms (Martin and Parkhurst, 2004) and small embryonic wounds displayed the characteristic concentric rings of actin fibres and activated (phosphorylated) non-muscle myosin at the wound edges (Fig. 2A). A similar concentric actomyosin ring at the wound edge was observed in small wounds of adult zebrafish, in addition to general cortical actomyosin formation in first-row keratinocytes possibly involved in other morphogenetic processes (Kim and Davidson, 2010) (Fig. 2B). By contrast, wound-facing domains of LE keratinocytes of larger partial-thickness wounds displayed an arrayed pattern of actin, which is characteristic of lamellipodial protrusions, whereas myosin was concentrated more posteriorly (Fig. 2C,D), another characteristic of migrating cells. Additionally, especially during the unilateral re-epithelialization of full-thickness wounds, the LE increased its width while spreading over the wound (Movie 1), whereas during purse-string driven concentric closure, the LE should become smaller. Together, this points to the existence of active keratinocyte migration during cutaneous wound closure in adult zebrafish, whereas purse-string mechanisms only occur in small wounds and, possibly, during the final steps of larger cutaneous wound closure.

To monitor cell migration processes at the LE, we performed high resolution *in vivo* imaging and scanning electron microscopy (SEM). Time-lapse imaging of partial-thickness wounds of *Tg(actb2:hras-egfp), Tg(krt4:mCherry)* double transgenic fish revealed that inner keratinocytes extended large, lamellipodia-like processes toward the centre of the wound and remained in close contact to each other, while superficial cells lagged behind (Fig. 2E-G; Movie 2). Basal epidermal cells behind the LE also formed cryptic lamellipodia (Fig. 2G, lower panel), as has been suggested previously from *in vitro* experiments (Matsubayashi et al., 2011). Only in rare cases did individual LE keratinocytes form lamellipodia that projected beyond the otherwise homogeneous lamellipodial front (Fig. 2E) or even leave the epithelial sheet entirely (Fig. 2H). Altogether, this behaviour of LE keratinocytes is very similar to the collective 'lamellipodial crawling' observed in scratch wound assays of confluently cultured keratinocytes (Fenteany et al., 2000). Protrusive activity at the LE was also present in early-stage full-thickness wounds, when re-epithelializing keratinocytes were still on the surface of naked scale remnants (Fig. S2A,B), whereas during later stages, when LE keratinocytes had reached regions where the wounds were deeper (see Fig. 1C), no such protrusions were observed (Fig. S2C,D).

The following epidermis: radial intercalation, cellular flattening, directed elongation and tissue recruitment from inter-scale pockets

Striking morphological changes were also observed in the epidermis at a distance from the wound. At 4 h post wounding (hpw), the epidermis immediately adjacent to the LE of full-thickness wounds had become thinner and bi-layered (Fig. 3A,B,E,F), displaying a similar organization to the neo-epidermis on the wound bed (Fig. 1F-H). In more remote regions (2 mm distance), the epidermis displayed normal thickness and multi-layered
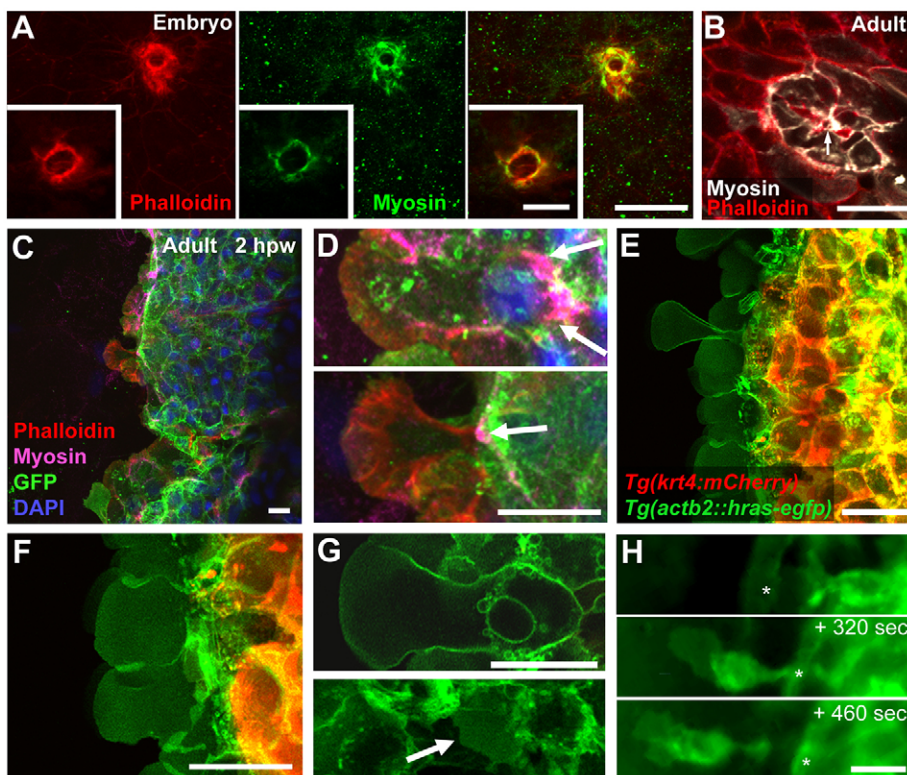

Fig. 2. LE cells of partial-thickness wounds form lamellipodia but lack signs of purse-string mechanisms. (A) Puncture wound in fin of 3-day-old embryo shows circular, colocalized actin (left panel) and phosphorylated non-muscle myosin (middle panel) at the wound margin. Images are maximum projections, insets single z-planes in the centre of the wound. (B) Puncture wound in trunk of adult, with cortical p-myosin in adjacent keratinocytes, including the sides facing the wound (arrow). (C,D) Adult partial-thickness wound; actin fibres are present within the protruding lamellipodia (red), p-myosin is accumulated at the posterior of LE cells (magenta, arrow). (E-G) Live confocal images of partial-thickness wound of *Tg(actb2:hras-egfp), Tg(krt4:mCherry)* double transgenic. Lamellipodia are formed at the LE by inner keratinocytes (green), whereas superficial cells (red) remain further back (E,F). (G) Single plane confocal images, revealing the enormous lamellipodial size relative to the cell body of an LE keratinocyte (upper panel). Inner keratinocytes behind the LE also show restricted protrusive activity (G, bottom panel; lamellipodium, arrow). (H) Stills from a time-lapse movie at indicated relative time points. Rarely, usually when encountering an obstruction, LE cells undergo more pronounced EMT-like changes and retain only limited contact with following cells. Asterisks indicate the same blood vessel. Scale bars: 20 μm in A-H; 10 μm in insets in A.
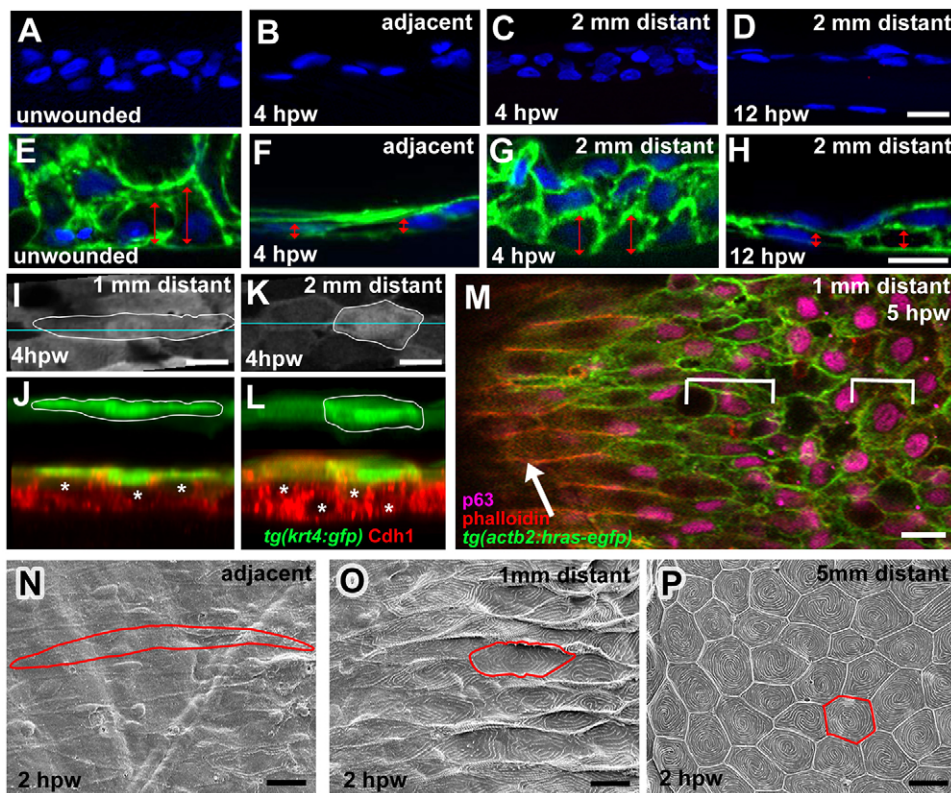
Fig. 3. Epidermal cells outside full-thickness wounds undergo progressive radial intercalation, flattening and elongation. (A-D) DAPI labelling of sections through unwounded epidermis (A) and epidermis at indicated stages and distances from wound (B-D). (E-H) DAPI labelling of sections through *Tg(actb2:hras-egfp)* fish as in A-D. Cell membranes are in green. Doubled-headed red arrows indicate the heights of individual basal keratinocytes. (I-L) Surface views (I,K) and z-projections (J,L) of *Tg(krt4:GFP)* fish; at 1 mm distance, superficial cells (outlined; green) display more pronounced flattening, and inner keratinocytes (E-cadherin; red; centres indicated by asterisks) more pronounced radial intercalations than at 2 mm distance from wound. (M) Single-plane confocal micrograph of *Tg(actb2:hras-egfp)* fish; superficial cells are labelled with Phalloidin (red), inner epidermal cells with p63 (pink) and cell membranes with GFP (green); wound is to the left. Arrow indicates superficial cells, brackets indicate lengths of inner keratinocytes, which are less elongated than superficial cells. (N-P) SEM images of superficial skin layer (single cells outlined) at indicated distances from wound, revealing spatially graded cell elongation and loss of surface microridges. Scale bars: 10 µm.

organization at 4 hpw, but was also thinner and bi-layered at 12 hpw (Fig. 3C,D). Apoptosis of keratinocytes as a cause of this thinning is unlikely, because no TUNEL^{+} cells could be detected in the epidermis around the wound (Fig. S3). Rather, it seems to be driven by progressive cell flattening (Fig. 3E-L) and by radial intercalations between basal and suprabasal keratinocytes (Fig. 3J,L; see also below). Analysis of *Tg(krt4:gfp)* fish (Fig. 3I-L) and SEM analysis (Fig. 3N-P) further revealed a progressive elongation of cells. As in unwounded skin, superficial cells at a 5 mm distance from the wound displayed a hexagonal shape (Fig. 3P). However, closer to the wound they were strongly elongated in the direction of the wound and displayed a progressive loss of surface microridges, although epithelial integrity was maintained (Fig. 3N,O). Inner keratinocytes also underwent directed elongations, however, to a lesser extent than in the superficial layer (Fig. 3M).

The cell shape changes in superficial cells outside the wound were also reflected by a progressive fading of the GFP fluorescence in superficial views of *Tg(krt4:GFP)* fish, encompassing regions up to 2 mm around the entire circumference of the wound at 5 hpw (Fig. S4A). Furthermore, the affected domain had lost the brighter fluorescence normally present in distal-most regions of the scales (Fig. S4A), reflecting the presence of epidermal pockets between adjacent scales (Fig. S4A, inset). These epidermal pockets are connected to the basal dermis via dermal tethers (Richardson et al., 2013), which in regions around the wound were stretched, whereas the pocket epidermis had moved up (Fig. S4B-E). This suggests that the inter-scale pockets serve as a reservoir of epidermal tissue that is recruited during wound re-epithelialization. Consistently, wounds on the forehead, which lacks scales, closed more slowly (Fig. S1D). Even more strongly reduced closure rates (~100 µm/h) were observed in the flank of *edar* mutants (Fig. S4F-H), which lack scales due to a genetic blockage of scale induction (Harris et al.,

2008). Of note, head wounds of *edar* mutants closed with similar rates as in wild-type siblings (Fig. S4I,J), suggesting that the reduced closure rates of trunk wounds in *edar* mutants are indeed due to the absence of the inter-scale pockets, rather than defects in epidermal cells themselves.

Re-epithelialization requires rearrangements of the actin cytoskeleton and TGF-β/integrin and Rock/JNK activities

To elucidate the molecular mechanisms of re-epithelialization, we treated wounded adult zebrafish with different specific inhibitors: cytochalasin D, a potent inhibitor of actin polymerization (Casella et al., 1981); the TGF-β signalling inhibitor SB431542 (Inman et al., 2002), which upon application to early gastrula embryos induced phenotypes similar to those displayed by mutants in the TGF-β family members Ndr1 and Ndr2 (Fig. S5A,B; Feldman et al., 1998); RGD peptides competing with the respective ECM integrin ligands of the migration substrate (Kim et al., 1992), which have been formerly shown to abrogate multiple fibronectin-integrin-dependent morphogenetic processes during early zebrafish development (Matsui et al., 2007; Nair and Schilling, 2008; Jülich et al., 2009); the Jun N-terminal kinase (JNK; Mapk8b – Zebrafish Information Network) inhibitor SP600125 (Bennett et al., 2001), which led to a significant reduction of pJNK levels in western blot analyses of extracts from adult skin (Fig. S5C); or Y27632 and inhibitor III Rockout, specific inhibitors of Rho-associated kinase (Rock), a crucial mediator of the small GTPase Rho during its regulation of actin cytoskeleton dynamics (Yarrow et al., 2005; Lai et al., 2005; Weiser et al., 2007). All inhibitors tested resulted in significantly slower re-epithelialization of partial thickness wounds (Fig. 4A), whereas closure of full-thickness wounds was significantly compromised upon cytochalasin D treatment and inhibition of Rock and JNK, but not following inhibition of TGF-β signalling (Fig. 4B). However, for both wound
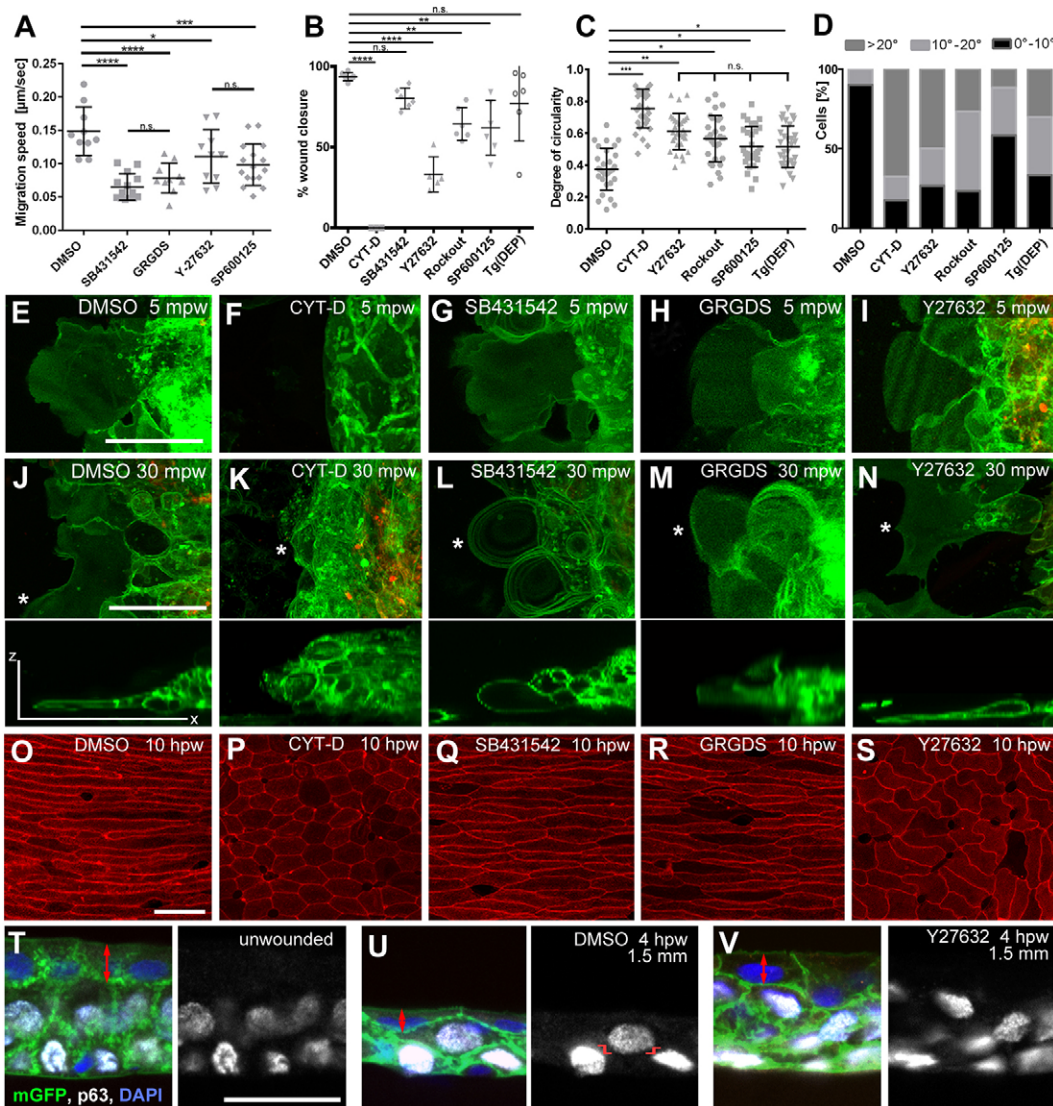
DEVELOPMENT

Fig. 4. Re-epithelialization requires TGF-β/GRGDS-dependent keratinocyte crawling at the LE and Rock/JNK-dependent epithelial morphogenesis in the following epidermis. (A-D) Quantification of effects caused by the indicated inhibitors on LE migration speeds in partial-thickness wounds (A), and on the extent of wound closure (B), the degree of circularity (C) and the orientation of the long axis (D) of adjacent superficial cells of full-thickness wounds at 10 hpw. Tg(DEP), transgenic inhibition of PCP. In A-C, mean values and s.d. are indicated. Values in A were determined from time-lapse movies (e.g. Movies 2-5; $n \geq 5$ per condition), values in B from Methylene Blue penetration assays as shown in Fig. S4F,G, and values in C,D from images as shown in O-S. *$P<0.05$; **$P<0.01$; ***$P<0.005$; ****$P<0.001$; n.s., not significant; one-way ANOVA with a Dunnett's post-hoc test. (E-N) Live confocal images of the LE of *Tg(actb2:hras-egfp), Tg(krt4:mCherry)* double transgenic fish at 5 min (E-I) and 30 min (J-N) after partial-thickness wounding (mpw), treated with indicated inhibitors. Lower panels of J-N show *z*-projections of the LE cell marked by the asterisk in the panels above. At 5 mpw, all cases except the CYT-D treatment display normal protrusive activity at the LE, whereas at 30 mpw, SB431542- and GRGDS-treated LE keratinocytes display roundish, shorter and thicker lamellipodia, indicative of lamellipodial retraction. (O-S) Phalloidin staining of the adjacent epidermis of full-thickness wounds at 10 hpw demonstrating compromised and uncoordinated cell elongation upon treatment with CYT-D (P) and Y27632 (S), but not SB431542 (Q) or GRGDS (S). (T-V) p63, GFP double immunofluorescence and DAPI labelling of sections through *Tg(actb2:hras-egfp)* fish at indicated conditions and distances from full-thickness wounds. Left panels, merge; right panels, p63 channels. Y27632-treated wound (V) displays reduced flattening of superficial cells (double-headed red arrows) and reduced frequency of radial intercalations, characterized by a partial overlap of the positions along the epidermal apical-basal axis occupied by adjacent basal and suprabasal p63[+] nuclei (marked in U by red lines). Quantifications from three individual fish per condition (1-1.5 mm wound distance for U,V) yielded the following frequencies (no. of partially overlapping p63[+] nuclei/total no. of p63[+] nuclei). Unwounded in T, 6.1±5.3%; DMSO-treated wound in U, 51.3±3.7%; Y27632-treated wound in V, 17.2±4.9%. $P=0.00027557$ (T versus U); $P=0.056567873$ (T versus V); $P=0.000651499$ (U versus V); Student's *t*-test. Scale bars: 20 μm.

types, completely arrested closure was only obtained by cytochalasin D treatment (Fig. 4B,F,K), suggesting that different actin cytoskeleton remodelling processes are at play that are differentially targeted by the other inhibitors.

Effects on cellular behaviour were studied by *in vivo* imaging of keratinocytes at the LE of partial-thickness wounds (Fig. 4E-N and Movie 2) or Phalloidin labelling of the actin cytoskeleton in superficial cells of the following epidermis of full-thickness wounds

(Fig. 4O-S). After control DMSO treatment, keratinocytes at the LE underwent active cell migration (Fig. 4E,J), whereas following cells elongated drastically (Fig. 4C,O). Cytochalasin D treatment, which blocked re-epithelialization completely, led to a loss of lamellipodia formation at the LE (Fig. 4F,K), whereas following cells maintained their hexagonal epithelial organization, as in unwounded skin (Fig. 4C,P). Upon TGF-β signalling inhibition, lamellipodia at the LE were initially formed normally (Fig. 4G);

however, they later acquired more roundish shapes and collapsed (Fig. 4L), while forward cellular movement was compromised (Fig. 4A; Movies 3 and 4). By contrast, elongation of more-distant cells was unaffected by the failure of lamellipodial crawling at the LE (Fig. 4Q and Fig. S6). Very similar, but slightly weaker lamellipodial and keratinocyte migration defects were obtained upon treatment with RGD peptides (Fig. 4A,H,M; Movie 5). Together, this suggests that TGF-β signalling is required for proper lamellipodial substrate attachment and crawling of keratinocytes at the LE.

Rock inhibition did not affect lamellipodial shape and stability at the LE, and cells migrated in a less co-ordinated manner, projecting into different directions (Fig. 4I,N). Similarly, cells of the following epidermis did undergo cell shape changes and elongated. However, compared with DMSO-treated, TGF-β-inhibited or RGD-treated fish (Fig. 4C,D,O,Q,S), their elongation was less pronounced (Fig. 4C,S) and less directed (Fig. 4D,S). Similar effects were obtained upon inhibition of JNK (Fig. 4C,D).

Consistent with the effect on directed keratinocyte elongation, JNK and Rock have been described as components of the planar cell polarity (PCP) pathway (Marlow et al., 2002; Munoz-Soriano et al., 2012; Seo et al., 2010). Accordingly, upon treatment of gastrulating embryos, SP600125, Y27632 and Rockout caused convergent extension defects (Fig. S7A-E) resembling those of mutants in other components of the PCP pathway (Marlow et al., 2002). In addition, the inhibitors led to compromised enveloping layer (EVL) and deep cell epiboly events (Fig. S8A-F) driven by flattening of superficial EVL cells and radial intercalations among deep cells (Warga and Kimmel, 1990; Slanchev et al., 2009), which are thus morphogenetic processes, as also evident in the following epidermis of adult wounds (see above; Fig. 3). Therefore, as a more specific approach to investigate the impact of PCP on wound closure, we generated a transgenic line expressing the DEP (Dishevelled, Egl-10 and Pleckstrin) domain of Dishevelled under the control of a heat-inducible hsp70 promoter for temporally controlled PCP pathway inhibition. Activation of the transgene during gastrulation caused convergent extension defects as obtained upon chemical Rock or JNK inhibition (Fig. S7F). However, despite strongly induced transgene expression (Fig. S7G-K), closure of adult full-thickness wounds was not significantly reduced compared with non-transgenic siblings (Fig. 4B; $P=0.144$), although effects on keratinocyte elongation and directionality were of similar strength as upon inhibition of Rock or JNK (Fig. 4C,D). This suggests that in addition to establishing proper PCP, Rock and JNK promote re-epithelialization via other morphogenetic processes. Indeed, Rock inhibition led to reduced flattening of superficial keratinocytes and reduced radial intercalation frequencies between basal and intermediary keratinocytes in the following epidermis (Fig. 4T-V), combined with reduced levels and an altered subcellular distribution of phosphorylated non-muscle myosin (Fig. S8G,H). Together, this suggests that Rock and JNK regulate multiple myosin-dependent rearrangements of keratinocytes in the following epidermis that are required for their collective displacement towards and onto the wound.

Re-epithelialization does not require keratinocyte proliferation

Keratinocyte proliferation is dispensable for wound closure in mammalian embryos (Ihara and Motobayashi, 1992), but is required for wound re-epithelialization in adult mammals, with inhibition or upregulation of this cellular process resulting in delayed or enhanced wound closure, respectively (Han et al., 2011; Tscharntke et al., 2007; Zhang et al., 2011). Histological analysis

of the neo-epidermis of zebrafish wounds revealed a highly thickened neo-epidermis covering the wound at both 24 and 72 hpw, with up to 10 cell layers (Fig. 5A), whereas unwounded epidermis consists of 3-4 layers (Richardson et al., 2013). However, at 24 hpw, the epidermis at 1 and 2 mm distant from the wound was thinner and consisted of two cell layers, whereas it had recovered to its normal thickness at 72 hpw (Fig. 5B,C). Analysis of BrdU incorporation demonstrated an absence of cell proliferation within the wound epidermis during the first 24 hpw, when re-epithelialization occurs (Fig. 5D), and rather moderate labelling at 48 and 72 hpw (Fig. 5E,F). By contrast, high and progressively increasing cell proliferation rates were observed in the epidermis at a 1 mm distance from the wound (Fig. 5G-I). This suggests that keratinocyte proliferation is dispensable for wound re-epithelialization, but required for the recovery of normal epidermal thickness in adjacent regions, from which keratinocytes have been recruited to the neo-epidermis during wound closure. Consistent with this notion, treatment of wounded zebrafish with hydroxyurea, an inhibitor of cell proliferation, had no effect on re-epithelialization rates (Fig. 5J,K) and the thickness of the neo-epidermis in the wounded region (Fig. 5L,M), whereas the adjacent epidermis remained bi-layered even at 72 hpw (Fig. 5N,O).

Transgenic inhibition of FGF signalling does not compromise wound re-epithelialization, but results in reduced keratinocyte proliferation and compromised epidermal regrowth

It has been shown that transgenic expression of a dominant-negative version of the FGF receptor FGFR2IIIb in keratinocytes compromises wound closure in adult mouse models (Werner et al., 1994). We have previously used a similar approach in transgenic *Tg(hsp70l:dnfgfr1-EGFP)* zebrafish, which upon heat-shock application express a C-terminally truncated mutant form of Fgfr1a in which the cytoplasmic tyrosine kinase domain is replaced by GFP. This truncated version is predicted to heterodimerise with, and to thereby block all FGF receptor subtypes (Lee et al., 2005; Lepilina et al., 2006). Activation of this transgene resulted in the almost complete failure of granulation tissue formation beneath the wound (Richardson et al., 2013). However, wounds of heat-shocked *Tg(hsp70l:dnfgfr1-EGFP)* fish re-epithelialized at the same rate as in controls (Fig. 6A-D), with a normally stratified neo-epidermis evident at 24 hpw (Fig. 6E,F). Furthermore, LE protrusive activity appeared unaffected by blockage of FGF signalling (compare Fig. 6L with Fig. 4E), altogether pointing to unaltered wound re-epithelialization. By contrast, the epidermis at a 1 mm distance from the wound failed to regenerate to its normal thickness (Fig. 6G,H) and the number of BrdU-incorporating cells in the epidermis around the wound remained significantly reduced, even at 4 days after wounding (Fig. 6I-K), similar to the defects obtained upon hydroxyurea treatment (see above; Fig. 5). Together, this indicates that FGF signalling plays no essential motogenic role, but rather has an essential mitogenic role, being required for keratinocyte proliferation to govern the regrowth of the adjacent epidermis after re-epithelialization is complete.

DISCUSSION
Re-epithelialization of adult fish wounds combines mechanisms used during wound closure in embryonic and adult mammals

In mouse embryos, wound closure involves coordinated, actomyosin-dependent purse-string contractions in LE keratinocytes, whereas active keratinocyte migration is required for wound closure in adult
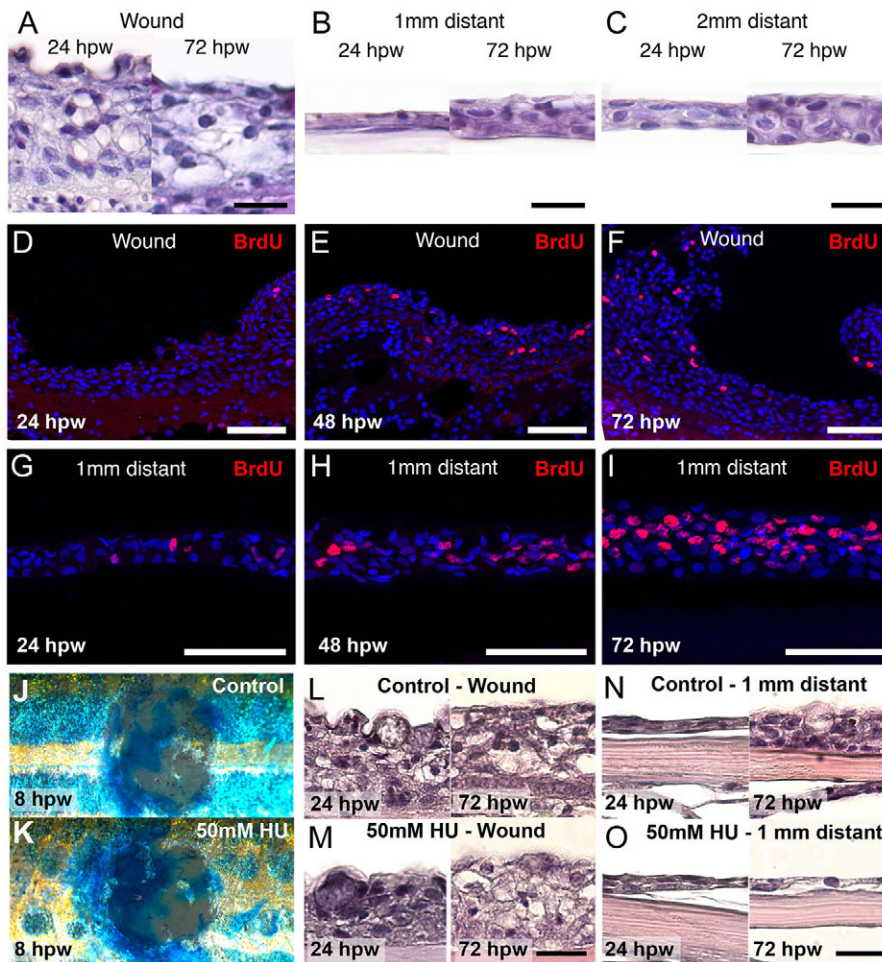
Fig. 5. Epidermal cell proliferation regenerates the surrounding epidermis but does not influence re-epithelialization. (A-C) Histological analysis reveals a highly thickened neo-epidermis at both 24 and 72 hpw (A). The epidermis 1 mm (B) and 2 mm (C) distant to the wound is much thinner at 24 hpw, but has recovered to normal thickness by 72 hpw. (D-I) BrdU-incorporation studies reveal few labelled cells in the wound epidermis from 24 hpw to 72 hpw (D-F), but a strong increase of BrdU^{+} cells in the epidermis 1 mm distant from the wound (G-I). (J-O) Fish treated with hydroxyurea (HU) exhibit the same rate of re-epithelialization as assessed by Methylene Blue assay at 8 hpw (J,K). Histological analysis between control and HU-treated fish reveals similar epidermal thicknesses in the wound at 24 hpw and 72 hpw (L,M), and 1 mm distant from the wound at 24 hpw (N,O). However, at 72 hpw, the latter has recovered to its normal thickness in the control, but remains thin in the HU-treated fish (N,O). Scale bars: 20 μm in A-C, L-O; 50 μm in D-J.

mice. Several growth factors have been identified that can promote keratinocyte migration, such as TGF-β1 (Gailit et al., 1994; Zambruno et al., 1995), EGF (Haase et al., 2003), macrophage-stimulating protein (MSP) (Santoro et al., 2003) and hepatocyte growth factor/scatter factor (HGF/SF) (Chmielowiec et al., 2007), which stimulate EMT of keratinocytes by regulating integrin transmembrane receptors and/or small GTPases, thereby modulating cell-ECM interactions and the actin cytoskeleton, respectively. In healing wounds of adult zebrafish, we observed keratinocytes with mesenchymal-like shapes and the presence of filopodia and lamellipodia at the LE of the re-epithelializing epidermal tongue, indicative of (partial) EMT and active cell migration (Fig. 2 and Fig. S2), and consistent with the recent observation in large wounds of zebrafish embryos (Gault et al., 2014). Furthermore, inhibition of TGF-β signalling and interference with integrin-ECM binding compromised lamellipodial shape and stability, as well as re-epithelialization rates (Fig. 4). Strikingly, these effects were most pronounced in partial thickness wounds, which in contrast to full-thickness wounds, retain a basal dermal layer as a potential substrate for efficient keratinocyte migration, consistent with previous reports suggesting that TGF-β overexpression in mouse accelerates closure of only partial-thickness wounds (Tredget et al., 2005). Together, this suggests that, as in mammals, re-epithelialization of wounds of adult zebrafish involves integrin-dependent lamellipodial crawling of keratinocytes at the LE.

In cultured epithelial cells, closure of scratched wounds is not only achieved by activities at the front row, but also involves several rows of following epithelial cells that migrate as coherent cell sheets

(Farooqui and Fenteany, 2005; Fenteany et al., 2000; Matsubayashi et al., 2011). We observed a similar phenomenon in keratinocytes following the LE in zebrafish wounds *in vivo*, with (cryptic) lamellipodia also formed by second and third row keratinocytes (Fig. 2G). In addition, we observed several other types of epithelial rearrangements that are not re-capitulated in the scratch assays. First, inner keratinocytes behind the LE undergo radial intercalations, which lead to a progressive reduction of cell layers and a concomitant two-dimensional growth of the remaining layers, thereby supplying the keratinocytes to cover the wound independent of cell proliferation (Figs 3 and 4). This is very similar to the radial intercalations driving deep cell epiboly in gastrulating embryos (Warga and Kimmel, 1990) and to the 'leap-frog' mechanism formerly described for the initiation of re-epithelialization at the LE of cutaneous wounds in the cichlid fish *Hemichromis bimaculatus* (Quilhac and Sire, 1999). However, our data show that these intercalations occur over a much broader temporal and spatial range, progressively (within hours) spreading into regions quite remote from the wound (distance larger than wound diameter). In addition, keratinocytes undergo directed and coordinated cell flattening, polarization and elongation (Fig. 3; Movie 4). This behaviour is most pronounced in the superficial layer, which apparently does not participate in the intercalation movements, but also takes place, to a lesser extent, in the deeper layers.

Chemical treatments indicate that the coordinated alignment of elongated cells as well as their radial intercalation and wound re-epithelialization depend on Rock and JNK activity (Fig. 4). Inhibition of Rho kinase has previously been shown to abrogate
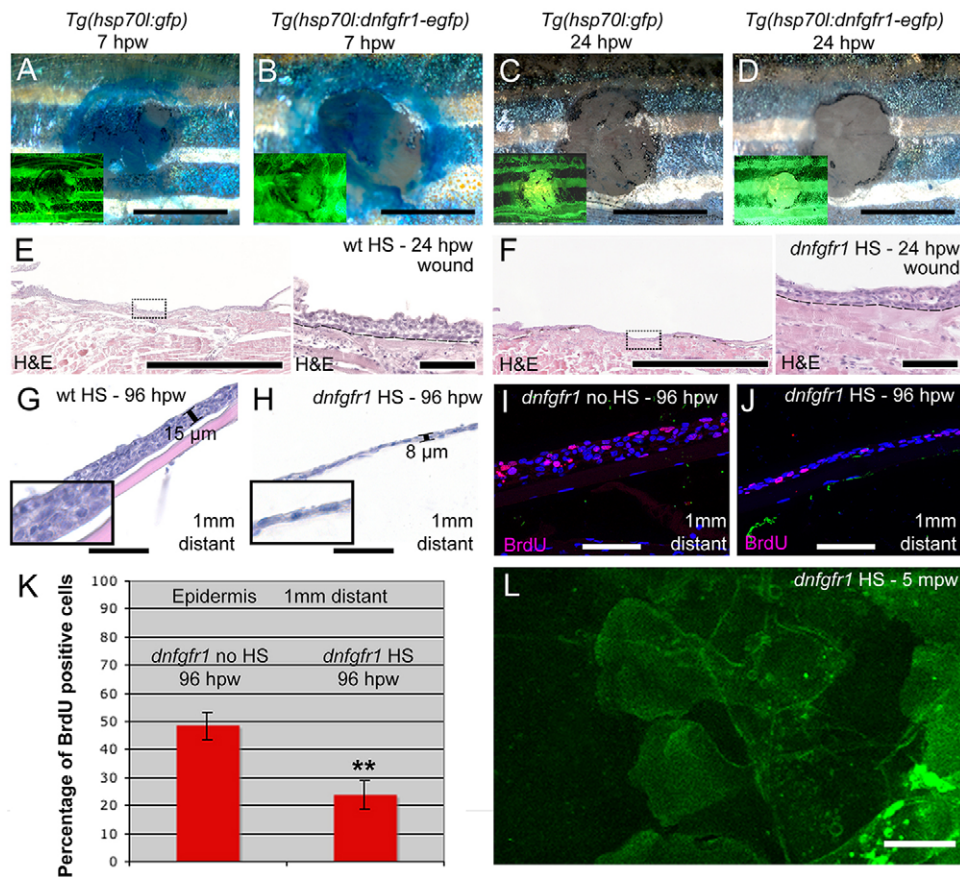
Fig. 6. FGF signalling is dispensable for re-epithelialization, but is required for keratinocyte proliferation and epidermal regrowth. (A-D) Methylene Blue penetration assay at 7 hpw (A,B) and 24 hpw (C,D) revealing unaltered re-epithelialization rates of full-thickness wounds between heat-shocked control Tg(*hsp70l:gfp*) (A,C) and *Tg(hsp70l:dnfgfr1-egfp)* (B,D). Insets show fluorescence of transgene-encoded GFP or dnFGFR-GFP fusion proteins, indicating strong transgene expression. (E,F) Histological analysis of wound epidermis at 24 hpw revealing unaltered thicknesses of neo-epidermis between heat-shocked wild-type control (E) and *Tg(hsp70l:dnfgfr1-egfp)* fish (F). Right panels show magnified views of regions boxed in left panels. (G,H) At 96 hpw, the epidermis 1 mm distant from the wound of the heat-shocked *Tg(hsp70l:dnfgfr1-egfp)* fish (H) is much thinner than in the heat-shocked non-transgenic control (G). Insets show magnified views. (I,J) BrdU incorporation revealing significantly reduced epidermal proliferation in heat-shocked (J) compared with non-heat shocked *Tg(hsp70l:dnfgfr1-egfp)* fish (I) 1 mm distant from the wound. (K) Quantification of BrdU incorporation rates (percentage of cells) from images as in I,J. (L) Live image of LE of heat-shocked *Tg(hsp70l:dnfgfr1-egfp)* fish after partial-thickness injury, revealing normal protrusive activity (see Fig. 4E as control). Scale bars: 2 mm in A-D; 500 μm in left panels of E,F; 50 μm in G-J and right panels of E,F; 10 μm in L.

purse string formation and thereby wound closure in fly and fish embryos (Abreu-Blanco et al., 2014; Gault et al., 2014). However, our analyses point to the absence of purse-string mechanisms during most closure phases of large cutaneous wounds in adult zebrafish, suggesting that other Rock-dependent processes must be affected. The identified requirement of Rock for proper non-muscle myosin activation/localization (Fig. S8), and for cell flattening and radial intercalations in the following epidermis (Fig. 4T-V) is in line with the formerly described myosin-II-dependent roles of Rock driving cell flattening during epidermal stratification in mammals (Vaezi et al., 2002) and radial cell intercalations during gut morphogenesis in Amphibia (Reed et al., 2009). In addition, Rock and JNK have been described as crucial components of the PCP pathway in multiple developmental contexts (Van Aelst and Symons, 2002). In zebrafish embryos, overexpression of a dominant-negative version of Rock2 results in compromised convergence extension movements, with cells elongating in rather random directions, rather than towards the midline, which is their supposed destination (Marlow et al., 2002). On the cellular level, these defects are very similar to those observed in the re-epithelializing epidermis after Rock and JNK inhibition. However, specific transgenic blockage of the PCP pathway affected wound closure much more moderately

than inhibition of Rock or JNK, although all treatments had comparable effects on directed keratinocyte elongation (Fig. 4). Together, this indicates that Rock and JNK regulate multiple morphogenetic movements, all of which might be myosin-dependent: cell flattening, radial cell intercalations and, as part of the PCP pathway, coordinated cell elongation. However, the latter seems to have a rather weak and, possibly, indirect impact on wound closure, promoting radial cell intercalations, which could be compromised when cells were elongated in random directions. Interestingly, similar cell elongations have been reported for superficial skin cells during wound closure in mouse, zebrafish and *Drosophila* embryos (Gault et al., 2014; Martin and Parkhurst, 2004; McCluskey and Martin, 1995; Razzell et al., 2014) and mutant analyses have unravelled an essential role of the PCP pathway for embryonic wound closure in mouse (Caddy et al., 2011).

Together, our data indicate that wound re-epithelialization of adult zebrafish uses a combination of mechanisms employed during embryonic and adult wound closure in mammals. Such an 'intermediary' nature of the mechanisms of re-epithelialization is consistent with the intermediary overall organization of the unwounded epidermis of adult zebrafish, resembling that of

mammalian embryos just before the onset of cornification (Fischer et al., 2014; Lee et al., 2014). In addition, our data indicate that in full-thickness zebrafish wounds, the major driving force of re-epithelialization is not generated by (TGF-β/RGD-dependent) active keratinocyte migration at the LE ('pulling at the front'), probably because of the absence of a suitable migration substrate, but rather by (Rock/JNK-dependent) epithelial rearrangements of keratinocytes further away from the wound ('pushing from the back'). By contrast, in partial-thickness wounds, both mechanisms are at play, explaining their higher closure rates (500 μm/h) compared with full-thickness wounds (250 μm/h). The even lower closure rates of cultured keratinocytes in scratch assays (50-70 μm/h) (Matsubayashi et al., 2011) might be due to the absence of such epithelial rearrangement further away from the LE, because here, cells are mono-layered and closure is solely dependent on active cell migration. Of note, this 'pushing' from the back, including the elongation/stretching of cells, seems to be largely independent of the 'pulling' at the front. Thus, in partial-thickness wounds, cell elongations in the following epidermis occur normally, even when lamellipodial crawling at the LE is blocked (Fig. S6). Similarly, keratinocytes in regions anterior of full-thickness wounds elongate and move forward, as in posterior regions (Fig. S1B,C; Movie 1), although the LE cannot reach the wound and cells pile up at the tip of the scales without any apparent contact to scale surfaces required for active migration on an ECM substrate (Fig. S1A). Future studies are required to reveal to what extent such pushing forces generated via long-range epithelial rearrangements further away from the LE also contribute to wound closure in adult mammals *in vivo*.

The zebrafish might assist in dissecting the different effects of growth factor signalling during mammalian wound healing

Direct comparisons of genetic control systems regulating *in vivo* re-epithelialization of fish and mammalian wounds are at first sight complicated by the differences in the time course with which the different steps of wound repair occur in the two vertebrate classes (Richardson et al., 2013). However, these differences, in combination with particular experimental strengths of the zebrafish system, might even help to dissect the described effects of different growth factors during mammalian wound closure at multiple levels. First, the temporal uncoupling of re-epithelialization from the other steps of wound healing helps to discriminate between direct/primary and indirect/secondary effects (e.g. via innate immune cells) on re-epithelializing keratinocytes. Second, the independence of re-epithelialization from keratinocyte proliferation (Fig. 5) helps to distinguish between motogenic and mitogenic effects. And third, the *in vivo* imaging of LE keratinocytes over several hours and at resolutions similar to those achieved in scratch assays *in vitro*, helps to distinguish between different cellular mechanisms underlying the motogenic effects.

During mouse wound repair, TGF-β fulfils multiple functions not only on keratinocytes, but also on other cell types involved in cutaneous wound repair. But even on keratinocytes, it has both a positive motogenic effect revealed *in vitro*, and a negative mitogenic effect revealed *in vivo* (see Introduction). In light of the positive *in vivo* effect of TGF-β on keratinocyte migration in zebrafish wounds revealed here (Fig. 4), it is tempting to speculate that despite the accelerated wound closure in mutant mice, TGF-β also has a positive effect on keratinocyte migration in closing mouse wounds *in vivo*, which is, however, overridden by other inhibitory effects, for instance on keratinocyte proliferation (Sivamani et al., 2007; Tredget et al., 2005).

Our data also allow first conclusions as to which particular processes of keratinocyte migration are regulated by TGF-β signalling. Re-epithelialization involves the dissociation of keratinocytes from the basement membrane zone at the undamaged wound margin, requiring the dissociation of hemidesmosomes and the formation of cellular protrusions pointing toward the wound. Subsequent directed migration over the wound bed requires the stimulation of focal adhesion proteins such as α5β1, α2β1, α3β1, αvβ5 and/or αvβ6 integrins, which mediate cell movement by the dynamic binding of extracellular matrix (ECM) components such as fibronectin and collagen to cell surfaces (Margadant and Sonnenberg, 2010; Tsuruta et al., 2011). Our chemical inhibitor experiments suggest that TGF-β signalling is dispensable for the protrusive activity of LE keratinocytes (Fig. 4), but is required for proper attachment of lamellipodia to the wound bed substrate and for keratinocyte migration. The latter are also sensitive to applied RGD peptides that are known to disrupt the physical interaction between RGD motif-containing ECM proteins and integrins (Fig. 4). This suggests that TGF-β promotes keratinocyte migration by modulating their integrin code, consistent with current concepts of TGF-β and integrin function in mammalian wound-healing systems (Fong et al., 2010; Gailit et al., 1994; Li et al., 2006; Margadant and Sonnenberg, 2010; Zambruno et al., 1995). Future zebrafish studies will reveal the nature of the relevant integrins and ECM proteins. In mammalian *in vitro* systems, RGD peptides selectively block the interaction of integrins with fibronectin (Kim et al., 1992), which might explain why in our *in vivo* assay, the effects of the RGD peptides were weaker than those obtained upon inhibition of TGF-β signalling (collagens, as alternative integrin ligands, should only be affected in the latter case) (Fig. 4). In addition, the relevant sources of the TGF-β signals need to be identified. Macrophages, a main source of TGF-β in mice, seem unlikely candidates, because re-epithelialization is initiated before inflammation (Richardson et al., 2013). Keratinocytes themselves might be a source, consistent with the reported TGF-β expression by keratinocytes of mammalian wounds (Schmid et al., 1993). In addition, injury might induce the release/activation of TGF-β stored in the ECM (Buscemi et al., 2011).

The aforementioned independence of re-epithelialization from keratinocyte proliferation in zebrafish might also underlie the seemingly different effects caused by loss of FGF signalling in zebrafish and mouse. In mouse, transgenic blockage of the FGF7/10/22 receptor FGFR2IIIb in keratinocytes results in decelerated wound closure (Werner et al., 1994). These defects could be due to decreased keratinocyte motility and/or proliferation, consistent with the migration-promoting effects revealed for FGF2 and FGF7/10 *in vitro*, and with their mitogenic effects demonstrated *in vivo* (auf demKeller et al., 2004; Sivamani et al., 2007; Werner et al., 1994). In contrast to mouse, *in vivo* blockage of FGF signalling in zebrafish affects neither wound re-epithelialization nor the protrusive activity of keratinocytes at the LE, suggesting that the motogenic function of FGF signalling is dispensable. However, treated fish do display significantly reduced proliferation rates of keratinocytes and failed regrowth of the adjacent epidermis to its normal thickness after wound closure is complete, pointing to an essential mitogenic effect of FGF signalling (Fig. 6). Together, this suggests that the cellular mechanisms of FGF signalling during wound re-epithelialization might be fully conserved between mammals and fish, and that the different net outcomes are solely due to the differential impacts of keratinocyte proliferation on wound closure in the different species.

MATERIALS AND METHODS

Zebrafish lines and wounding

Six- to twelve-month-old wild-type fish of the TL/Ekwill strain and the following published mutant and transgenic lines were used for adult wounding experiments: $edar^{z3R367W}$ (Harris et al., 2008), $Tg(actb2:hras-egfp)vu119$, $Tg(krt4:egfp)gz7$, $Tg(hsp70l:EGFP)$ and $Tg(hsp70l:dnfgfr1-EGFP)pd1$ (Cooper et al., 2005; Gong et al., 2002; Halloran et al., 2000; Lee et al., 2005). The $Tg(krt4:mCherry)fr32$ line and the $Tg(hsp70l:DEP)fr37$ line, containing the $Xenopus$ Dishevelled DEP domain (aa 371-736; Tada and Smith, 2000), were generated using the gateway-based Tol2 kit (Kwan et al., 2007), followed by standard injection procedures.

Puncture wounds in embryonic median fins were manually introduced with a glass needle; puncture wounds in adult fish with a micro-point nitrogen ablation laser (Andor). Full-thickness wounds of adult fish (Richardson et al., 2013) with a diameter of ∼2 mm (unless stated otherwise) were introduced with a Dermablate laser, as described (trunk: 2 pulses at 500 mJ; head: 1 pulse at 400 mJ). For partial-thickness wounds, adult fish were anaesthetized in 0.13% Tricaine (w/v) and a scale removed manually with forceps. Adult $Tg(hsp70l:dnfgfr1-egfp)$ and $Tg(hsp70l:DEP)$ fish were heat-shocked at 40°C for 1 h in pre-warmed water, then returned to 27°C water and wounded 1 h later.

All zebrafish experiments were approved by the National Animal Welfare Committee (LANUV Nordrhein-Westfalen; 8.87-50.10.31. 08.134; 84-02.04.2012.A251; 84-02.04.2012.A253; City of Cologne; 576.1.36.6.3.01.10 Be).

Tissue labelling procedures

The Methylene Blue penetration assay and histological and immunofluorescence analyses were performed as described (Richardson et al., 2013). For Fig. 3E-H, $Tg(actb2:hras-egfp)$ fish were fixed with 4% paraformaldehyde (PFA) overnight at 4°C, followed by cryosectioning and mounting of sections in Mowiol (Carl Roth) containing DAPI. Primary antibodies/labelling reagents used were: p63 (1:100, Santa Cruz, sc-8431), chicken anti-GFP (1:100, Invitrogen, A10262), phospho-myosin light chain 2 (Ser19) (1:100, Cell Signaling, 3671), E-cadherin (1:200, BD Biosciences, 610182), Rhodamine-Phalloidin (1:100, Invitrogen, R415). Epidermal cell proliferation was assessed by incubating adult fish in 100 µg/ml BrdU (Sigma) for 12 h prior to and specified times post wounding. BrdU water was exchanged every 24 h. TUNEL staining of apoptotic cells (Fischer et al., 2014), and $myoD$ and $Xenopus DEP$ (Tada and Smith, 2000) whole-mount $in situ$ hybridizations were carried out as described (Hammerschmidt et al., 1996). Images were captured on a Zeiss Axiophot, Zeiss Apotome, Zeiss Confocal (LSM710 META) or Leica M165 FC dissecting microscope. SEM analysis was carried out as described (Fischer et al., 2014).

Drug treatments

Adult zebrafish were treated with 2 µM cytochalasin D (CYT-D; Sigma, C8273), 50 µM Y27632 (Calbiochem, 688000), 50 µM Rho Kinase Inhibitor III, Rockout (Calbiochem, 55553), 50 µM SB431542 (Sigma, S4317), 1 mM GRGDS peptide (Bachem, H1345), 10 µM SP600125 (Sigma, S5567) or 50 mM hydroxyurea (Calbiochem, 400046) in fish system water. Fish were treated starting 4 h prior to wounding and inhibitors were refreshed every 24 h when necessary. Efficacies of SB431542, Y27632, Rockout and SP600125 were tested in parallel treatments or microinjections (Y27632; Lai et al., 2005; Lou et al., 2012) of zebrafish embryos, analysing convergent extension by $myoD in situ$ hybridization (Fig. S7), and epiboly and mesoderm formation by morphological inspection or Phalloidin staining, as described (Slanchev et al., 2009) (Figs S5 and S8).

In vivo imaging

Time-lapse $in vivo$ imaging of re-epithelializing partial- or full-thickness wounds of adult zebrafish was carried out on a Zeiss Apotome as described (Xu et al., 2014) with the following modifications: fish were anaesthetized with 0.016% Tricaine and mounted in a home-made imaging chamber using 2% low-melting point agarose. The chamber was connected to a peristaltic pump (Gilson Minipuls 3), which provided an inflow and outflow of 0.016% Tricaine in system water in a circulatory manner. Agarose covering the gills and head was removed and fish were intubated with the inflow tube using a cut 200 µl pipette tip as a mouthpiece. The flow rate was set to ∼3 ml/min. The total volume of medium circulating in the system was generally 50 ml, but 500 ml was used for long-term imaging (>2 h). Images were processed using ImageJ (NIH) and its 'extended depth of field' plug-in, as described (Forster et al., 2004).

Quantification and statistics

For Fig. 4A-D, at least six individual fish, or ten individual cells from at least three individual fish were analysed using ImageJ software. Data collection and analysis was conducted with Microsoft Excel 2010 and GraphPad Prism6. For statistical analysis, mean values were determined for each analysed wound, if necessary, and then used as data points to determine mean values and standard deviations for all analysed wounds (n) with Student's t-test or one-way ANOVA followed by a Dunnett's post-hoc test. Data for which representative images are shown without statistical calculations were obtained from at least six out of six investigated specimens from at least three independent experiments.

References

Abreu-Blanco, M. T., Verboon, J. M. and Parkhurst, S. M. (2014). Coordination of Rho family GTPase activities to orchestrate cytoskeleton responses during cell wound repair. *Curr. Biol.* **24**, 144-155.

Ashcroft, G. S., Yang, X., Glick, A. B., Weinstein, M., Letterio, J. L., Mizel, D. E., Anzano, M., Greenwell-Wild, T., Wahl, S. M., Deng, C. et al. (1999). Mice lacking Smad3 show accelerated wound healing and an impaired local inflammatory response. *Nat. Cell Biol.* **1**, 260-266.

auf demKeller, U., Krampert, M., Kümin, A., Braun, S. and Werner, S. (2004). Keratinocyte growth factor: effects on keratinocytes and mechanisms of action. *Eur. J. Cell Biol.* **83**, 607-612.

Barrientos, S., Stojadinovic, O., Golinko, M. S., Brem, H. and Tomic-Canic, M. (2008). Growth factors and cytokines in wound healing. *Wound Repair Regen.* **16**, 585-601.

Bement, W. M., Forscher, P. and Mooseker, M. S. (1993). A novel cytoskeletal structure involved in purse string wound closure and cell polarity maintenance. *J. Cell Biol.* **121**, 565-578.

Bennett, B. L., Sasaki, D. T., Murray, B. W., O'Leary, E. C., Sakata, S. T., Xu, W., Leisten, J. C., Motiwala, A., Pierce, S., Satoh, Y. et al. (2001). SP600125, an anthrapyrazolone inhibitor of Jun N-terminal kinase. *Proc. Natl. Acad. Sci. USA* **98**, 13681-13686.

Brock, J., Midwinter, K., Lewis, J. and Martin, P. (1996). Healing of incisional wounds in the embryonic chick wing bud: characterization of the actin purse-string and demonstration of a requirement for Rho activation. *J. Cell Biol.* **135**, 1097-1107.

DEVELOPMENT

Buscemi, L., Ramonet, D., Klingberg, F., Formey, A., Smith-Clerc, J., Meister, J.-J. and Hinz, B. (2011). The single-molecule mechanics of the latent TGF-beta1 complex. *Curr. Biol.* **21**, 2046-2054.

Caddy, J., Wilanowski, T., Darido, C., Dworkin, S., Ting, S. B., Zhao, Q., Rank, G., Auden, A., Srivastava, S., Papenfuss, T. A. et al. (2011). Epidermal wound repair is regulated by the planar cell polarity signaling pathway. *Dev. Cell* **19**, 138-147.

Casella, J. F., Flanagan, M. D. and Lin, S. (1981). Cytochalasin D inhibits actin polymerization and induces depolymerization of actin filaments formed during platelet shape change. *Nature* **293**, 302-305.

Chmielowiec, J., Borowiak, M., Morkel, M., Stradal, T., Munz, B., Werner, S., Wehland, J., Birchmeier, C. and Birchmeier, W. (2007). c-Met is essential for wound healing in the skin. *J. Cell Biol.* **177**, 151-162.

Cooper, M. S., Szeto, D. P., Sommers-Herivel, G., Topczewski, J., Solnica-Krezel, L., Kang, H.-C., Johnson, I. and Kimelman, D. (2005). Visualizing morphogenesis in transgenic zebrafish embryos using BODIPY TR methyl ester dye as a vital counterstain for GFP. *Dev. Dyn.* **232**, 359-368.

Cowin, A. J., Brosnan, M. P., Holmes, T. M. and Ferguson, M. W. J. (1998). Endogenous inflammatory response to dermal wound healing in the fetal and adult mouse. *Dev. Dyn.* **212**, 385-393.

Farooqui, R. and Fenteany, G. (2005). Multiple rows of cells behind an epithelial wound edge extend cryptic lamellipodia to collectively drive cell-sheet movement. *J. Cell Sci.* **118**, 51-63.

Feldman, B., Gates, M. A., Egan, E. S., Dougan, S. T., Rennebeck, G., Sirotkin, H. I., Schier, A. F. and Talbot, W. S. (1998). Zebrafish organizer development and germ-layer formation require nodal-related signals. *Nature* **395**, 181-185.

Fenteany, G., Janmey, P. A. and Stossel, T. P. (2000). Signaling pathways and cell mechanics involved in wound closure by epithelial cell sheets. *Curr. Biol.* **10**, 831-838.

Fischer, B., Metzger, M., Richardson, R., Knyphausen, P., Ramezani, T., Franzen, R., Schmelzer, E., Bloch, W., Carney, T. J. and Hammerschmidt, M. (2014). p53 and TAp63 promote keratinocyte proliferation and differentiation in breeding tubercles of the zebrafish. *PLoS Genet.* **10**, e1004048.

Fong, E., Tzlil, S. and Tirrell, D. A. (2010). Boundary crossing in epithelial wound healing. *Proc. Natl. Acad. Sci. USA* **107**, 19302-19307.

Forster, B., Van De Ville, D., Berent, J., Sage, D. and Unser, M. (2004). Complex wavelets for extended depth-of-field: a new method for the fusion of multichannel microscopy images. *Microsc. Res. Tech.* **65**, 33-42.

Gailit, J., Welch, M. P. and Clark, R. A. F. (1994). TGF-beta 1 stimulates expression of keratinocyte integrins during re-epithelialization of cutaneous wounds. *J. Invest. Dermatol.* **103**, 221-227.

Gault, W. J., Enyedi, B. and Niethammer, P. (2014). Osmotic surveillance mediates rapid wound closure through nucleotide release. *J. Cell Biol.* **207**, 767-782.

Gong, Z., Ju, B., Wang, X., He, J., Wan, H., Sudha, P. M. and Yan, T. (2002). Green fluorescent protein expression in germ-line transmitted transgenic zebrafish under a stratified epithelial promoter from keratin8. *Dev. Dyn.* **223**, 204-215.

Haase, I., Evans, R., Pofahl, R. and Watt, F. M. (2003). Regulation of keratinocyte shape, migration and wound epithelialization by IGF-1- and EGF-dependent signalling pathways. *J. Cell Sci.* **116**, 3227-3238.

Halloran, M. C., Sato-Maeda, M., Warren, J. T., Su, F., Lele, Z., Krone, P. H., Kuwada, J. Y. and Shoji, W. (2000). Laser-induced gene expression in specific cells of transgenic zebrafish. *Development* **127**, 1953-1960.

Hammerschmidt, M., Pelegri, F., Mullins, M. C., Kane, D. A., Brand, M., van Eeden, F. J. M., Furutani-Seiki, M., Granato, M., Haffter, P., Heisenberg, C. P. et al. (1996). Mutations affecting morphogenesis during gastrulation and tail formation in the zebrafish, Danio rerio. *Development* **123**, 143-151.

Han, G., Li, F., Ten Dijke, P. and Wang, X. J. (2011). Temporal smad7 transgene induction in mouse epidermis accelerates skin wound healing. *Am. J. Pathol.* **179**, 1768-1779.

Harris, M. P., Rohner, N., Schwarz, H., Perathoner, S., Konstantinidis, P. and Nüsslein-Volhard, C. (2008). Zebrafish eda and edar mutants reveal conserved and ancestral roles of ectodysplasin signaling in vertebrates. *PLoS Genet.* **4**, e1000206.

Hopkinson-Woolley, J., Hughes, D., Gordon, S. and Martin, P. (1994). Macrophage recruitment during limb development and wound healing in the embryonic and foetal mouse. *J. Cell Sci.* **107**, 1159-1167.

Ihara, S. and Motobayashi, Y. (1992). Wound closure in foetal rat skin. *Development* **114**, 573-582.

Inman, G. J., Nicolas, F. J., Callahan, J. F., Harling, J. D., Gaster, L. M., Reith, A. D., Laping, N. J. and Hill, C. S. (2002). SB-431542 is a potent and specific inhibitor of transforming growth factor-beta superfamily type I activin receptor-like kinase (ALK) receptors ALK4, ALK5, and ALK7. *Mol. Pharmacol.* **62**, 65-74.

Jülich, D., Mould, A. P., Koper, E. and Holley, S. A. (2009). Control of extracellular matrix assembly along tissue boundaries via Integrin and Eph/Ephrin signaling. *Development* **136**, 2913-2921.

Kim, H. Y. and Davidson, L. A. (2010). Punctuated actin contractions during convergent extension and their permissive regulation by the non-canonical Wnt-signaling pathway. *J. Cell Sci.* **124**, 635-646.

Kim, J. P., Zhang, K., Kramer, R. H., Schall, T. J. and Woodley, D. T. (1992). Integrin receptors and RGD sequences in human keratinocyte migration: unique anti-migratory function of alpha 3 beta 1 epiligrin receptor. *J. Invest. Dermatol.* **98**, 764-770.

Koch, R. M., Roche, N. S., Parks, W. T., Ashcroft, G. S., Letterio, J. J. and Roberts, A. B. (2000). Incisional wound healing in transforming growth factor-beta1 null mice. *Wound Repair Regen.* **8**, 179-191.

Kwan, K. M., Fujimoto, E., Grabher, C., Mangum, B. D., Hardy, M. E., Campbell, D. S., Parant, J. M., Yost, H. J., Kanki, J. P. and Chien, C.-B. (2007). The Tol2kit: a multisite gateway-based construction kit for Tol2 transposon transgenesis constructs. *Dev. Dyn.* **236**, 3088-3099.

Lai, S.-L., Chang, C.-N., Wang, P.-J. and Lee, S.-J. (2005). Rho mediates cytokinesis and epiboly via ROCK in zebrafish. *Mol. Reprod. Dev.* **71**, 186-196.

Lamouille, S., Xu, J. and Derynck, R. (2014). Molecular mechanisms of epithelial–mesenchymal transition. *Nat. Rev. Mol. Cell Biol.* **15**, 178-196.

Lee, Y., Grill, S., Sanchez, A., Murphy-Ryan, M. and Poss, K. D. (2005). Fgf signaling instructs position-dependent growth rate during zebrafish fin regeneration. *Development* **132**, 5173-5183.

Lee, R. T. H., Asharani, P. V. and Carney, T. J. (2014). Basal keratinocytes contribute to all strata of the adult zebrafish epidermis. *PLoS ONE* **9**, e84858.

Lepilina, A., Coon, A. N., Kikuchi, K., Holdway, J. E., Roberts, R. W., Burns, C. G. and Poss, K. D. (2006). A dynamic epicardial injury response supports progenitor cell activity during zebrafish heart regeneration. *Cell* **127**, 607-619.

Li, Y., Fan, J., Chen, M., Li, W. and Woodley, D. T. (2006). Transforming growth factor-alpha: a major human serum factor that promotes human keratinocyte migration. *J. Invest. Dermatol.* **126**, 2096-2105.

Longaker, M. T., Whitby, D. J., Adzick, N. S., Crombleholme, T. M., Langer, J. C., Duncan, B. W., Bradley, S. M., Stern, R., Ferguson, M. W. J. and Harrison, M. R. (1990). Studies in fetal wound healing, VI. Second and early third trimester fetal wounds demonstrate rapid collagen deposition without scar formation. *J. Pediatr. Surg.* **25**, 63-69.

Lou, Q., He, J., Hu, L. and Yin, Z. (2012). Role of lbx2 in the noncanonical Wnt signaling pathway for convergence and extension movements and hypaxial myogenesis in zebrafish. *Biochem. Biophys. Acta* **1823**, 1024-1032.

Margadant, C. and Sonnenberg, A. (2010). Integrin–TGF-beta crosstalk in fibrosis, cancer and wound healing. *EMBO Rep.* **11**, 97-105.

Marlow, F., Topczewski, J., Sepich, D. and Solnica-Krezel, L. (2002). Zebrafish Rho kinase 2 acts downstream of Wnt11 to mediate cell polarity and effective convergence and extension movements. *Curr. Biol.* **12**, 876-884.

Martin, P. (1997). Wound healing–aiming for perfect skin regeneration. *Science* **276**, 75-81.

Martin, P. and Lewis, J. (1992). Actin cables and epidermal movement in embryonic wound healing. *Nature* **360**, 179-183.

Martin, P. and Parkhurst, S. M. (2004). Parallels between tissue repair and embryo morphogenesis. *Development* **131**, 3021-3034.

Matsubayashi, Y., Razzell, W. and Martin, P. (2011). 'White wave' analysis of epithelial wound healing reveals how cells mobilise back from the leading edge in a myosin-II-dependent fashion. *J. Cell Sci.* **124**, 1017-1021.

Matsui, T., Raya, A., Callol-Massot, C., Kawakami, Y., Oishi, I., Rodriguez-Esteban, C. and Izpisúa Belmonte, J. C. (2007). miles-apart-mediated regulation of cell–fibronectin interaction and myocardial migration in zebrafish. *Nat. Clin. Pract. Cadiovasc. Med.* **4** Suppl. 1, S77-S82.

McCluskey, J. and Martin, P. (1995). Analysis of the tissue movements of embryonic wound healing—DiI studies in the limb bud stage mouse embryo. *Dev. Biol.* **170**, 102-114.

Meyer, M., Muller, A.-K., Yang, J., Moik, D., Ponzio, G., Ornitz, D. M., Grose, R. and Werner, S. (2012). FGF receptors 1 and 2 are key regulators of keratinocyte migration in vitro and in wounded skin. *J. Cell Sci.* **125**, 5690-5701.

Munoz-Soriano, V., Belacortu, Y. and Paricio, N. (2012). Planar cell polarity signaling in collective cell movements during morphogenesis and disease. *Curr. Genomics* **13**, 609-622.

Nair, S. and Schilling, T. F. (2008). Chemokine signaling controls endodermal migration during zebrafish gastrulation. *Science* **322**, 89-92.

Presland, R. B. and Jurevic, R. J. (2002). Making sense of the epithelial barrier: what molecular biology and genetics tell us about the functions of oral mucosal and epidermal tissues. *J. Dent. Educ.* **66**, 564-574.

Quilhac, A. and Sire, J.-Y. (1999). Spreading, proliferation, and differentiation of the epidermis after wounding a cichlid fish, Hemichromis bimaculatus. *Anat. Rec.* **254**, 435-451.

Räsänen, K. and Vaheri, A. (2010). TGF-beta1 causes epithelial-mesenchymal transition in HaCaT derivatives, but induces expression of COX-2 and migration only in benign, not in malignant keratinocytes. *J. Dermatol. Sci.* **58**, 97-104.

Razzell, W., Wood, W. and Martin, P. (2014). Recapitulation of morphogenetic cell shape changes enables wound re-epithelialisation. *Development* **141**, 1814-1820.

Reed, R. A., Womble, M. A., Dush, M. K., Tull, R. R., Bloom, S. K., Morckel, A. R., Devlin, E. W. and Nascone-Yoder, N. M. (2009). Morphogenesis of the primitive gut tube is generated by Rho/Rock/Myosin II-mediated endoderm rearrangements. *Dev. Dyn.* **238**, 3111-3125.

Richardson, R., Slanchev, K., Kraus, C., Knyphausen, P., Eming, S. and Hammerschmidt, M. (2013). Adult zebrafish as a model system for cutaneous wound-healing research. *J. Invest. Dermatol.* **133**, 1655-1665.

Santoro, M. M. and Gaudino, G. (2005). Cellular and molecular facets of keratinocyte reepithelization during wound healing. *Exp. Cell Res.* **304**, 274-286.

Santoro, M. M., Gaudino, G. and Marchisio, P. C. (2003). The MSP receptor regulates alpha6beta4 and alpha3beta1 integrins via 14-3-3 proteins in keratinocyte migration. *Dev. Cell* **5**, 257-271.

Schmid, P., Cox, D., Bilbe, G., McMaster, G., Morrison, C., Stähelin, H., Lüscher, N. and Seiler, W. (1993). TGF-betaS and TGF-beta type II receptor in human epidermis: differential expression in acute and chronic skin wounds. *J. Pathol.* **171**, 191-197.

Seo, J., Asaoka, Y., Nagai, Y., Hirayama, J., Yamasaki, T., Namae, M., Ohata, S., Shimizu, N., Negishi, T., Kitagawa, D. et al. (2010). Negative regulation of wnt11 expression by Jnk signaling during zebrafish gastrulation. *J. Cell Biochem.* **110**, 1022-1037.

Shaw, T. J. and Martin, P. (2009). Wound repair at a glance. *J. Cell Sci.* **122**, 3209-3213.

Singer, A. J. and Clark, R. A. F. (1999). Cutaneous wound healing. *N. Engl. J. Med.* **341**, 738-746.

Sivamani, R. K., Garcia, M. S. and Isseroff, R. R. (2007). Wound re-epithelialization: modulating keratinocyte migration in wound healing. *Front. Biosci.* **12**, 2849-2868.

Slanchev, K., Carney, T. J., Stemmler, M. P., Koschorz, B., Amsterdam, A., Schwarz, H. and Hammerschmidt, M. (2009). The epithelial cell adhesion molecule EpCAM is required for epithelial morphogenesis and integrity during zebrafish epiboly and skin development. *PLoS Genet.* **5**, e1000563.

Tada, M. and Smith, J. C. (2000). XWnt11 is a target of Xenopus Brachyury: regulation of gastrulation movements via Dishevelled, but not through the canonical Wnt pathway. *Development* **127**, 2227-2238.

Tredget, E. B., Demare, J., Chandran, G., Tredget, E. E., Yang, L. and Ghahary, A. (2005). Transforming growth factor-beta and its effect on reepithelialization of partial-thickness ear wounds in transgenic mice. *Wound Repair Regen.* **13**, 61-67.

Tscharntke, M., Pofahl, R., Chrostek-Grashoff, A., Smyth, N., Niessen, C., Niemann, C., Hartwig, B., Herzog, V., Klein, H. W., Krieg, T. et al. (2007). Impaired epidermal wound healing in vivo upon inhibition or deletion of Rac1. *J. Cell Sci.* **120**, 1480-1490.

Tsuruta, D., Hashimoto, T., Hamill, K. J. and Jones, J. C. (2011). Hemidesmosomes and focal contact proteins: functions and cross-talk in keratinocytes, bullous diseases and wound healing. *J. Dermatol. Sci.* **62**, 1-7.

Vaezi, A., Bauer, C., Vasioukhin, V. and Fuchs, E. (2002). Actin cable dynamics and Rho/Rock orchestrate a polarized cytoskeletal architecture in the early steps of assembling a stratified epithelium. *Dev. Cell* **3**, 367-381.

Van Aelst, L. and Symons, M. (2002). Role of Rho family GTPases in epithelial morphogenesis. *Genes Dev.* **16**, 1032-1054.

Warga, R. M. and Kimmel, C. B. (1990). Cell movements during epiboly and gastrulation in zebrafish. *Development* **108**, 569-580.

Weber, C. E., Li, N. Y., Wai, P. Y. and Kuo, P. C. (2012). Epithelial-mesenchymal transition, TGF-beta, and osteopontin in wound healing and tissue remodeling after injury. *J. Burn Care Res.* **33**, 311-318.

Weiser, D. C., Pyati, U. J. and Kimelman, D. (2007). Gravin regulates mesodermal cell behavior changes required for axis elongation during zebrafish gastrulation. *Genes Dev.* **21**, 1559-1571.

Werner, S. and Grose, R. (2003). Regulation of wound healing by growth factors and cytokines. *Physiol. Rev.* **83**, 835-870.

Werner, S., Smola, H., Liao, X., Longaker, M. T., Krieg, T., Hofschneider, P. H. and Williams, L. T. (1994). The function of KGF in morphogenesis of epithelium and reepithelialization of wounds. *Science* **266**, 819-822.

Xu, C., Hasan, S. S., Schmidt, I., Rocha, S. F., Pitulescu, M. E., Bussmann, J., Meyen, D., Raz, E., Adams, R. H. and Siekmann, A. F. (2014). Arteries are formed by vein-derived endothelial tip cells. *Nat. Commun.* **5**, 5758.

Yarrow, J. C., Totsukawa, G., Charras, G. T. and Mitchison, T. J. (2005). Screening for cell migration inhibitors via automated microscopy reveals a Rho-kinase inhibitor. *Chem. Biol.* **12**, 385-395.

Zambruno, G., Marchisio, P. C., Marconi, A., Vaschieri, C., Melchiori, A., Giannetti, A. and De Luca, M. (1995). Transforming growth factor-beta 1 modulates beta 1 and beta 5 integrin receptors and induces the de novo expression of the alpha v beta 6 heterodimer in normal human keratinocytes: implications for wound healing. *J. Cell Biol.* **129**, 853-865.

Zhang, M., Liu, N.-Y., Wang, X.-E., Chen, Y.-H., Li, Q.-L., Lu, K.-R., Sun, L., Jia, Q., Zhang, L. and Zhang, L. (2011). Activin B promotes epithelial wound healing in vivo through RhoA-JNK signaling pathway. *PLoS ONE* **6**, e25143.

DEVELOPMENT